

Lipid Acyl Chain *cis* Double Bond Position Modulates Membrane Domain Registration/Anti-Registration

Siya Zhang^{†,‡} and Xubo Lin^{*,†,§}

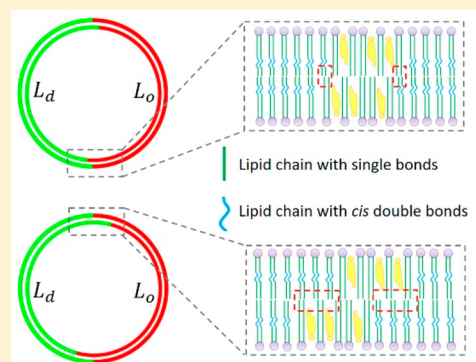
[†]Institute of Nanotechnology for Single Cell Analysis (INSCA), Beijing Advanced Innovation Center for Biomedical Engineering, Beihang University, Beijing 100191, China

[‡]State Key Laboratory of Medical Molecular Biology, School of Basic Medicine, Peking Union Medical College and Institute of Basic Medical Sciences, Chinese Academy of Medical Sciences, Beijing 100005, China

[§]School of Biological Science and Medical Engineering, Beihang University, Beijing 100191, China

Supporting Information

ABSTRACT: *Inter-leaflet* coupling is critical to control the dynamics of membrane domain registration/anti-registration, which is important in maintaining proper biological functions. Factors such as lipid acyl chain inter-digitation and membrane remodeling have been found to be able to regulate the *inter-leaflet* coupling. However, detailed molecular mechanisms that dominate the *inter-leaflet* coupling are still far from clear. Here, we revealed that lipid acyl chain *cis* double bond position can regulate the *inter-leaflet* coupling according to our coarse-grained and all-atom molecular dynamics simulations. The farther the double bond is away from the lipid tail terminal, the weaker the *inter-leaflet* attractive interactions between unsaturated lipids. Therefore, the relative motions of membrane domains in two membrane leaflets become more obvious (membrane domain anti-registration). Generally, our simulations validated a direct indicator for the *inter-leaflet* coupling strength, which provides physical insights into the molecular mechanisms of membrane domain registration/anti-registration.



INTRODUCTION

The plasma membrane contains various lipids and proteins, which play critical roles in many biological processes such as the selective permeability and the signal transduction.¹ It has been generally agreed that the plasma membrane can segregate into functional and dynamic nanoscale membrane domains due to differential interactions between lipids and proteins, where the functional liquid-ordered (L_o) domains are termed as “lipid rafts”.^{2–4} These ordered membrane domains are tightly correlated to many biological functions of the plasma membrane.^{4,5} In order to reveal these correlations, many efforts have been made to understand the dynamics of the lipid raft and its effects on proteins. Consensus has been achieved that lipid unsaturation difference as well as the presence of cholesterol molecules serve as a prerequisite for the formation of lipid rafts.^{6–8} The lipid chain order difference between raft and nonraft domains provides a better quantitative indicator to evaluate the domain stability of the lipid raft than the domain thickness difference.^{9–11} Besides, this domain stability can further affect the stability of membrane-bound proteins (e.g., H-Ras nanocluster^{12–14}) as well as the raft affinity of transmembrane proteins.^{15–17} It is worth mentioning that the domain stability discussed above mainly refers to the *inner-leaflet* domain dynamics. Since the lipid raft domains in two opposite leaflets of a lipid bilayer can have relative motions, in other words, the raft domain stability should consist of both

inner-leaflet and *inter-leaflet* domain dynamics.¹⁸ Compared to the *inner-leaflet* domain dynamics, the *inter-leaflet* domain dynamics is still far from clear.

Membrane domain registration and anti-registration describe the *inter-leaflet* domain dynamics,^{19,20} which are mainly determined by the *inter-leaflet* coupling^{18,21} and may play an important role in regulating membrane-mediated signal transductions.^{22,23} Generally, the *inter-leaflet* coupling can be modulated by lipid acyl chain inter-digitation^{18,24–26} and membrane remodeling induced by external forces.^{27–30} However, quantifications of lipid acyl chain inter-digitations in either model membranes or plasma membranes are not easy for molecular experiments. Besides, it is still a challenge to directly study the *inter-leaflet* domain dynamics in molecular experiments, although it is possible to quantitatively tune the lipid composition in each membrane leaflet of asymmetric lipid vesicles.³¹ Hence, it will be very meaningful to identify a few measurable factors that are directly correlated to the *inter-leaflet* coupling with molecular simulations. However, for the two model membrane systems, if their *inner-leaflet* domain dynamics are quite different, it will be difficult to conclude whether the *inter-leaflet* domain dynamics is regulated by certain factors or just affected by different *inner-leaflet* domain

Received: July 1, 2019

Published: September 18, 2019

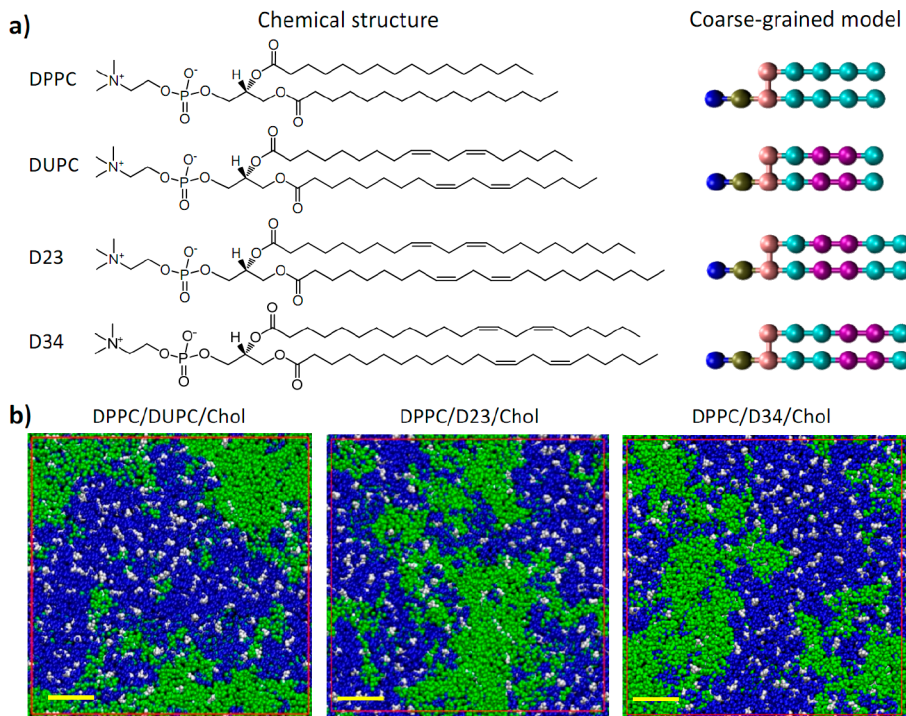


Figure 1. Description and visualization of our CGMD simulations: (a) The chemical structures and the corresponding CG models of phospholipids used in CGMD simulations. (b) Top-view snapshots of three model membrane systems at the end of 20 μ s CGMD simulations. DPPC is colored in blue, DUPC, D23, or D34 in green, and cholesterol in white. Scale bar: 3 nm.

dynamics. In other words, model membrane systems with similar *inner-leaflet* domain dynamics will be essential for the identification of these direct dominant factors. For example, the choice of sterols with different side chain lengths,^{32,33} which were reported to have little effects on the *inner-leaflet* domain dynamics in experiments,³⁴ can provide proper model systems to clarify the long-standing controversy^{35–37} on the role of cholesterol flip-flop in the membrane domain registration/anti-registration dynamics.

As discussed above, lipid unsaturation differences as well as cholesterol molecules are essential to the formation of the lipid raft^{7,8} and the *inner-leaflet* domain dynamics.^{9–11} And it has already been proved that cholesterol flip-flop is important in the membrane domain registration/anti-registration dynamics.^{32,33} However, whether lipid unsaturation can modulate the *inter-leaflet* domain dynamics or not is still unknown. Considering that there are various unsaturated lipids with ω -3, ω -6, and ω -9 fatty acid chains (where the distances between the *cis* double bond and lipid tail terminal are different) in the plasma membrane, we propose a hypothesis that unsaturated lipids with different acyl chain double bond positions may modulate the *inter-leaflet* coupling and thus *inter-leaflet* domain dynamics. To confirm this hypothesis, we studied the model membrane systems with only varied acyl chain double bond positions using molecular dynamics (MD) simulations, which is a useful tool to study the membrane domain dynamics.^{11,38–40} Our coarse-grained (CG) MD simulations indicated that the distance between the *cis* double bond and the lipid chain terminal determined the *inter-leaflet* coupling, which regulated the membrane domain registration/anti-registration. All-atom (AA) MD simulations of the model membrane including 1,2-dipalmitoyl-*sn*-glycero-3-phosphocholine (DPPC), 1,2-dioleoyl-*sn*-glycero-3-phosphocholine (DOPC), and 1,2-diarachidonoyl-*sn*-glycero-3-phosphocholine

(DAPC) further validated the results of CGMD simulations, our MD simulations confirmed that the lipid acyl chain *cis* double bond position could serve as a new direct indicator for the *inter-leaflet* coupling strength.

METHODS

CGMD Simulations. CG models,^{41–43} which allow MD simulations with much longer time-scale and larger length-scale, have been widely used to study the lipid raft dynamics in model membranes. In this work, we used the Martini CG model (version 2.1)⁴³ to probe the role of the lipid acyl chain *cis* double bond position in regulating the *inter-leaflet* coupling. 600 DPPC (di-16:0PC), 360 1,2-dilinoleoyl-*sn*-glycero-3-phosphocholine (DUPC or di-18:2PC)/di-22:2PC, 240 cholesterol (Chol), as well as 16134 water and 150 mM salt ions (Na^+ and Cl^-) were used for CGMD simulations. Here, we considered the two isomers of di-22:2PC with different *cis* double bond positions (Figure 1a), D23 and D34, which were supposed to have similar liquid phase separations and minimum hydrophobic mismatches between raft and nonraft domains. For CGMD simulations, a cutoff of 1.2 nm was used for van der Waals (vdW) interactions, and the Lennard-Jones potential was smoothly shifted to zero between 1.0 and 1.2 nm to reduce the cutoff noise. For electrostatic interactions, the Coulombic potential was smoothly shifted from 0 to 1.2 nm, with a cutoff at 1.2 nm. The default relative dielectric constant (15) of the force field was used in the simulations.⁴³ Lipids and water/ions were coupled separately to V-rescale heat baths⁴⁴ at $T = 298$ K (coupling constant $\tau = 1$ ps). The systems were simulated at 1 bar of pressure using a semi-isotropic Parrinello–Rahman pressure coupling scheme⁴⁵ with a coupling constant of $\tau = 5$ ps and compressibility of 3×10^{-4} bar⁻¹. The nonbonded interaction neighbor list was updated every 20 steps with a cutoff of 1.2 nm. Each simulation was run for 20 μ s with a time step of 20 fs.

AAMD Simulations. The CHARMM36m force field⁴⁶ was used to simulate the *inter-leaflet* domain dynamics of three-component model membranes with 120 DPPC, 120 DOPC, and 120 DAPC. The initial AAMD simulation system was built using the CHARMM-

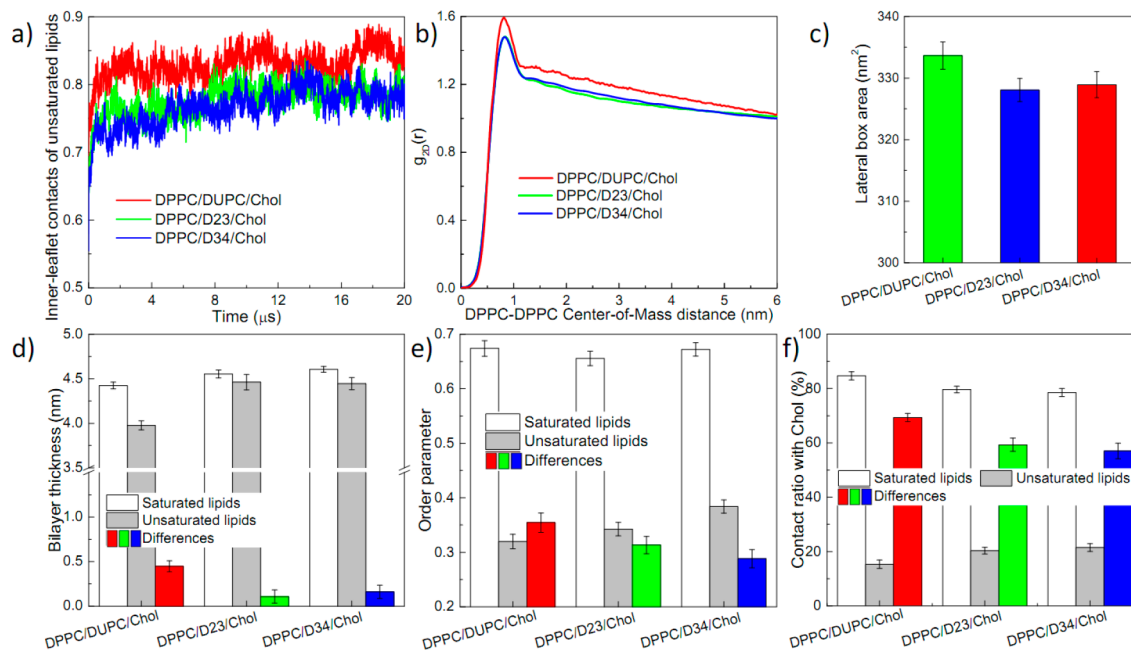


Figure 2. Quantitative analysis of CGMD simulations indicating that DPPC/D23/Chol and DPPC/D34/Chol have similar *inner-leaflet* domain dynamics: (a) Time evolution of inner-leaflet contacts of unsaturated lipids, which is normalized according to the pure lipid bilayer with the same number of unsaturated lipids. (b) DPPC–DPPC 2D radial distribution function profiles $g_{2D}(r)$ over DPPC–DPPC center-of-mass (COM) distances. Lateral box area (c), bilayer thickness (d), lipid chain order parameter (e), and cholesterol preference (f) for the three simulation systems (DPPC/D23/Chol, DPPC/D34/Chol, and DPPC/DUPC/Chol) were obtained based on the last 12 μ s of the 20 μ s CGMD simulations.

GUI.^{47,48} The Lennard-Jones potential was smoothly shifted to zero between 1.0 and 1.2 nm with a cutoff of 1.2 nm to reduce cutoff noise. Particle-mesh Ewald (PME) electrostatics⁴⁹ with a real space cutoff of 1.2 nm was used. Lipids and water/ions were coupled separately to Nosé–Hoover heat baths^{50,51} at $T = 298$ K (coupling constant $\tau = 1$ ps). The systems were simulated at 1 bar of pressure using a semi-isotropic Parrinello–Rahman pressure coupling scheme⁴⁵ with a coupling constant of $\tau = 5$ ps and compressibility of 4.5×10^{-5} bar⁻¹. Bonds with H atoms were constrained with the LINCS algorithm.⁵² The nonbonded interaction neighbor list was updated every 20 steps with a cutoff of 1.2 nm. The simulation was run for 1.4 μ s with a time step of 2 fs. Both CGMD and AAMD simulations were run with GROMACS software (version 2016.5).⁵³

RESULTS AND DISCUSSION

D23 and D34 Lipids Provide Ideal Model Membrane Systems for CGMD Simulations to Test the Role of Lipid Acyl Chain *cis* Double Bond Position in the *Inter-Leaflet* Domain Dynamics. In order to study lipid raft dynamics in CGMD simulations, the model membrane consisting of DPPC, DUPC, and cholesterol has been widely used,^{2,6,11,32} which provides useful physical insights into experiments with model membrane systems of more physiologically relevant lipids. It is widely reported that the DPPC/DUPC/Chol bilayer has stable phase separation and obvious thickness differences between L_o and liquid-disordered (L_d) domains.^{6,11} Considering that significant hydrophobic mismatches between L_o and L_d domains can promote membrane domain anti-registration,²⁸ we used longer unsaturated lipids (di-22:2PC) instead of DUPC in our CGMD simulations, which is supposed to have stable phase separation but little hydrophobic mismatch between L_o and L_d domains. Besides, we further used two isomers of di-22:2PC with different *cis* double bond positions: D23 and D34. The *cis* double bond is farther from the lipid tail terminal in D23 than that in D34 (Figure 1a). In other words, DPPC/D23/Chol and DPPC/D34/Chol may provide ideal

model systems to investigate the role of lipid acyl chain *cis* double bond position in regulating the *inter-leaflet* coupling. To make sure of this, we need to examine whether DPPC/D23/Chol and DPPC/D34/Chol have very similar *inner-leaflet* domain dynamics.

As shown in Figure 1b and Figure 2a,b, DPPC/D23/Chol and DPPC/D34/Chol have very similar phase separation evolution processes as well as membrane domain sizes/stability. Membrane domains in these two systems are less stable than those in DPPC/DUPC/Chol lipid bilayers. Besides, the lateral box areas are also very close, which indicates that DPPC/D23/Chol and DPPC/D34/Chol have similar membrane fluctuations (Figure 2c). Moreover, comparable differences of domain thicknesses (Figure 2d), lipid chain order parameters (Figure 2e), and cholesterol preferences (Figure 2f) further supported the aforementioned conclusion and validated that DPPC/D23/Chol and DPPC/D34/Chol have very similar *inner-leaflet* domain dynamics and thus were suitable for quantifying the role of lipid acyl chain *cis* double bond position in regulating *inter-leaflet* domain dynamics.

Lipid Acyl Chain *cis* Double Bond Position Modulates the *Inter-Leaflet* Domain Dynamics in CGMD Simulations. By using the two isomers of di-22:2PC (D23 and D34), we obtained two ideal model membrane systems, which have nearly the same *inner-leaflet* domain dynamics (Figure 2). Besides, thickness differences or hydrophobic mismatches between L_o and L_d domains have been greatly minimized. In our model membrane systems, we have excluded all of these factors that may affect the *inter-leaflet* domain dynamics. In other words, we can directly correlate the lipid acyl chain *cis* double bond position to the differences in *inter-leaflet* domain dynamics in these two model membrane systems. By analyzing the 2D probability density map of unsaturated lipid positions in both upper and lower membrane leaflets, we could clearly see a poor domain overlap between the two leaflets for the case

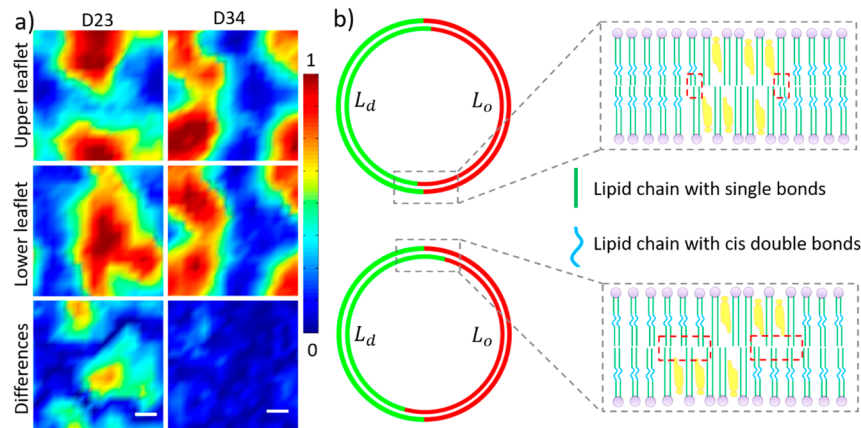


Figure 3. Lipid acyl chain *cis* double bond position can regulate inter-leaflet coupling and thus membrane domain registration/anti-registration: (a) Two-dimensional (2D) probability density map of unsaturated lipid positions for upper (top panel) and lower (middle panel) membrane leaflets over the last 4 μ s of the CGMD simulation trajectories. Their absolute differences (bottom panel) indicate that the lipid acyl chain *cis* double bond position determines the membrane domain registration/anti-registration processes. Scale bar: 3 nm. (b) Schematics for the underlying mechanism of this phenomenon.

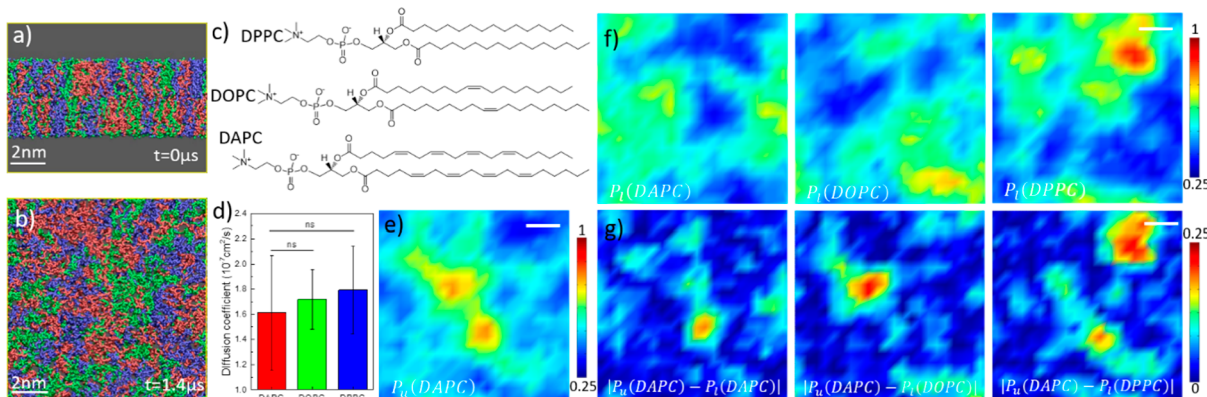


Figure 4. AAMD simulation of the DPPC/DOPC/DAPC symmetric lipid bilayer: (a) Side-view system snapshot at $t = 0 \mu\text{s}$. (b) Top-view system snapshot at $t = 1.4 \mu\text{s}$ indicated obvious clustering of lipids of the same type. DAPC is colored in red, DOPC in green, and DPPC in blue. For clarity, water and ions are not shown. (c) Chemical structures of DPPC, DOPC, and DAPC. The distance between the double bond and the lipid tail terminal is much larger in DOPC than that in DAPC. (d) Diffusion coefficients for DPPC, DOPC, and DAPC show no significant differences. (e) 2D probability density map for DAPC lipid positions in the upper membrane leaflet. (f) 2D probability density maps for DAPC, DOPC, and DPPC lipid positions in the lower lipid leaflet. (g) 2D probability density absolute difference maps between DAPC in the upper membrane leaflet and DAPC, DOPC, and DPPC in the lower leaflet. The analysis in parts d–g is based on the last 1 μs of the AAMD simulation trajectory.

of DPPC/D23/Chol (Figure 3a), which shows obvious membrane domain anti-registration. On the contrary, membrane domains in the two leaflets overlap very well and have almost complete registration in DPPC/D34/Chol. In other words, the lipid acyl chain *cis* double bond position directly regulates membrane domain registration/anti-registration.

As mentioned above, lipid tail *cis* double bonds play an important role in the formation of lipid rafts.^{4,6,11} It is the presence of these double bonds that induces the differential attractive interactions between saturated lipids, unsaturated lipids, and cholesterol,^{7,8} which drive the formation of lipid rafts. Especially, more preferred attractive interactions exist between unsaturated lipids. Within the same membrane leaflet, these lateral attractive interactions drive the liquid–liquid phase separation. Between the two membrane leaflets, these *inter-leaflet* attractive interactions will determine the *inter-leaflet* coupling. When *cis* double bonds in unsaturated lipids are far from the tail terminals (D23), contributions to the *inter-leaflet* attractive interactions from these *cis* double bonds will be greatly reduced. Thus, the *inter-leaflet* coupling will be

significantly weakened. Relative motions for membrane domains in the two leaflets become easier. Hence, membrane domain anti-registration appears. Our CGMD simulations demonstrate that the lipid acyl chain *cis* double bond position can serve as a direct indicator for the *inter-leaflet* coupling strength (Figure 3b), which determines the membrane domain registration/anti-registration.

AAMD Simulations Showed Consistent Results as CGMD Simulations. The Martini CG model maps several heavy atoms into one interaction site and thus allows the direct simulations of lipid rafts in much larger length scale and longer time scale.⁴³ In order to avoid the possible artifacts arising from this simplified treatment, we further tested the above conclusion using AAMD simulations and a DPPC/DOPC/DAPC model membrane (Figure 4a). We chose these three lipids because their CHARMM force field parameters are frequently validated in AAMD simulations.^{15,38} On the other hand, DPPC is a saturated lipid, while DOPC and DAPC are unsaturated lipids, which have ω -9 and ω -6 fatty acid tails (different *cis* double bond position), respectively (Figure 4c).

In this three-component lipid membrane, different lipids can form small clusters due to different attractive interactions between these lipids (Figure 4b). These lipids show similar and high diffusion abilities (Figure 4d), which enables the relative sufficient sampling in the AAMD simulation of the model membrane system and thus is suitable to test the conclusion obtained from the CGMD simulations. This is also the reason that we did not use cholesterol molecules in AAMD simulations. We then calculated the 2D probability density map of the DAPC position in the upper leaflet (Figure 4e) and the 2D probability density maps of DAPC, DOPC, and DPPC positions in the lower leaflet (Figure 4f). After calculating the absolute density difference maps between upper DAPC and lower DAPC, DOPC, and DPPC, it clearly shows that upper DAPC lipids have the best overlap degree with lower DAPC molecules and the worst overlap degree with lower DPPC lipids (Figure 4g). It fully indicates that the order of DAPC's preferred *inter-leaflet* attractive interactions is DAPC > DOPC > DPPC. In other words, both the presence of *cis* double bonds and their positions could affect the *inter-leaflet* coupling. It is worth mentioning that choosing lower DAPC molecules as the reference for 2D probability density map analysis has similar results as Figure 4. Our AAMD simulations pointed out the role of lipid chain *cis* double bond position in the *inter-leaflet* coupling, which validated the results of CGMD simulations.

As is known, the two membrane leaflets of the plasma membrane are tightly correlated to each other. When changes happen in one leaflet, the opposing leaflet responds correspondingly, which is critical for the exchange of biological signals. For example, Raghupathy et al. found that lipid clustering in the outer membrane leaflet can induce the corresponding lipid clustering in the inner leaflet and further promote the recruitment and clustering of lipid-anchored proteins.²² In other words, the *inter-leaflet* coupling plays a key role in these biological processes. As discussed above, the lipid chain inter-digititation is one direct factor that determines the *inter-leaflet* coupling in the condition of no external stress.^{18,26} However, it is not easy to evaluate the degree of the lipid chain inter-digititation in experiments. Hence, identifying parameters that are responsible for the *inter-leaflet* coupling and measurable in experiments will be important for understanding the detailed molecular mechanisms in plasma-membrane-related biological processes. Previous studies have pointed out that cholesterol dynamics can determine the *inter-leaflet* coupling and thus modulate the membrane domain registration/anti-registration.^{32,33,54} Here, we focused on the role of unsaturated lipids and found that changing lipid chain *cis* double bond positions in unsaturated lipids could significantly affect the *inter-leaflet* coupling according to MD simulations, which provided a new indicator for quantitatively assessing the *inter-leaflet* coupling strength.

CONCLUSION

In this work, by using model membrane systems where the lipid acyl chain *cis* double bond position is the only variable, we validate that the *cis* double bond position can serve as another direct dominant factor for the *inter-leaflet* coupling strength based on MD simulations. The farther the *cis* double bond is from the lipid tail terminal, the weaker the strength of *inter-leaflet* attractive interactions between unsaturated lipids and the smaller the differences between unsaturated–unsaturated and unsaturated–saturated *inter-leaflet* attractive interactions.

Hence, membrane domains in the two membrane leaflets can easily have relative motions in this case, which promotes the formation of membrane domain anti-registration.

ASSOCIATED CONTENT

Supporting Information

The Supporting Information is available free of charge on the ACS Publications website at DOI: 10.1021/jacs.9b06977.

Supplemental figures related to coarse-grained MD simulations of the lipid membrane systems including DPPC, hD23 or hD34, and cholesterol; coarse-grained MD simulations of the lipid membrane systems including DPPC, D12, D23, D34 or D45, and cholesterol; coarse-grained MD simulations of the thicker lipid membrane systems including DSPC, tD23 or tD34, and cholesterol; and membrane domain registration/anti-registration dynamics of the four lipid membrane systems including DPPC, D12, D23, D34, or D45, and cholesterol and table showing the lag time of the autocorrelation analysis (PDF)

AUTHOR INFORMATION

Corresponding Author

*linxbseu@buaa.edu.cn or linxbseu@163.com

ORCID

Xubo Lin: 0000-0002-4417-3582

Notes

The authors declare no competing financial interest.

ACKNOWLEDGMENTS

We thank Prof. Alemayehu Gorfe and Prof. Ilya Levental at UThealth for helpful discussions on lipid raft. This work was supported by the National Natural Science Foundation of China (No. 21903002), the Fundamental Research Funds for the Central Universities, and the startup funds of Beijing Advanced Innovation Center for Biomedical Engineering (X.L.). We thank the Supercomputing Center of Beihang University (512 CPU cores in total, open to the whole University) for generous computational resources.

REFERENCES

- (1) Van Meer, G.; Voelker, D. R.; Feigenson, G. W. Membrane Lipids: Where They Are and How They Behave. *Nat. Rev. Mol. Cell Biol.* **2008**, *9*, 112–124.
- (2) Cebecauer, M.; Amaro, M.; Jurkiewicz, P.; Sarmento, M. J.; Šachl, R.; Cwiklik, L.; Hof, M. Membrane Lipid Nanodomains. *Chem. Rev.* **2018**, *118*, 11259–11297.
- (3) Winkler, P. M.; Regmi, R.; Flauraud, V.; Brugger, J. r.; Rigneault, H.; Wenger, J. r. m.; García-Parajo, M. F. Transient Nanoscopic Phase Separation in Biological Lipid Membranes Resolved by Planar Plasmonic Antennas. *ACS Nano* **2017**, *11*, 7241–7250.
- (4) Sezgin, E.; Levental, I.; Mayor, S.; Eggeling, C. The Mystery of Membrane Organization: Composition, Regulation and Roles of Lipid Rafts. *Nat. Rev. Mol. Cell Biol.* **2017**, *18*, 361–374.
- (5) Simons, K.; Toomre, D. Lipid Rafts and Signal Transduction. *Nat. Rev. Mol. Cell Biol.* **2000**, *1*, 31–39.
- (6) Risselada, H. J.; Marrink, S. J. The Molecular Face of Lipid Rafts in Model Membranes. *Proc. Natl. Acad. Sci. U. S. A.* **2008**, *105*, 17367–17372.
- (7) Wang, C.; Krause, M. R.; Regen, S. L. Push and Pull Forces in Lipid Raft Formation: The Push Can Be as Important as the Pull. *J. Am. Chem. Soc.* **2015**, *137*, 664–666.

- (8) Wang, C.; Yu, Y.; Regen, S. L. Lipid Raft Formation: Key Role of Polyunsaturated Phospholipids. *Angew. Chem., Int. Ed.* **2017**, *56*, 1639–1642.
- (9) Levental, I.; Grzybek, M.; Simons, K. Raft Domains of Variable Properties and Compositions in Plasma Membrane Vesicles. *Proc. Natl. Acad. Sci. U. S. A.* **2011**, *108*, 11411–11416.
- (10) Heberle, F. A.; Petruzielo, R. S.; Pan, J.; Drazba, P.; Kučerka, N.; Standaert, R. F.; Feigenson, G. W.; Katsaras, J. Bilayer Thickness Mismatch Controls Domain Size in Model Membranes. *J. Am. Chem. Soc.* **2013**, *135*, 6853–6859.
- (11) Lin, X.; Lorent, J. H.; Skinkle, A. D.; Levental, K. R.; Waxham, M. N.; Gorfe, A. A.; Levental, I. Domain Stability in Biomimetic Membranes Driven by Lipid Polyunsaturation. *J. Phys. Chem. B* **2016**, *120*, 11930–11941.
- (12) Janosi, L.; Li, Z.; Hancock, J. F.; Gorfe, A. A. Organization, Dynamics, and Segregation of Ras Nanoclusters in Membrane Domains. *Proc. Natl. Acad. Sci. U. S. A.* **2012**, *109*, 8097–8102.
- (13) Li, Z.; Janosi, L.; Gorfe, A. A. Formation and Domain Partitioning of H-Ras Peptide Nanoclusters: Effects of Peptide Concentration and Lipid Composition. *J. Am. Chem. Soc.* **2012**, *134*, 17278–17285.
- (14) Lin, X.; Li, Z.; Gorfe, A. A. Reversible Effects of Peptide Concentration and Lipid Composition on H-Ras Lipid Anchor Clustering. *Biophys. J.* **2015**, *109*, 2467–2470.
- (15) Lin, X.; Gorfe, A. A.; Levental, I. Protein Partitioning into Ordered Membrane Domains: Insights from Simulations. *Biophys. J.* **2018**, *114*, 1936–1944.
- (16) Lin, X.; Gorfe, A. A. Understanding Membrane Domain-Partitioning Thermodynamics of Transmembrane Domains with Potential of Mean Force Calculations. *J. Phys. Chem. B* **2019**, *123*, 1009–1016.
- (17) Diaz-Rohrer, B. B.; Levental, K. R.; Simons, K.; Levental, I. Membrane Raft Association Is a Determinant of Plasma Membrane Localization. *Proc. Natl. Acad. Sci. U. S. A.* **2014**, *111*, 8500–8505.
- (18) Nickels, J. D.; Smith, J. C.; Cheng, X. Lateral Organization, Bilayer Asymmetry, and Inter-Leaflet Coupling of Biological Membranes. *Chem. Phys. Lipids* **2015**, *192*, 87–99.
- (19) van Meer, G. Dynamic Transbilayer Lipid Asymmetry. *Cold Spring Harbor Perspect. Biol.* **2011**, *3*, a004671.
- (20) Fujimoto, T.; Parmryd, I. Interleaflet Coupling, Pinning, and Leaflet Asymmetry—Major Players in Plasma Membrane Nano-domain Formation. *Front. Cell Dev. Biol.* **2017**, *4*, 155.
- (21) Fowler, P. W.; Williamson, J. J.; Sansom, M. S.; Olmsted, P. D. Roles of Interleaflet Coupling and Hydrophobic Mismatch in Lipid Membrane Phase-Separation Kinetics. *J. Am. Chem. Soc.* **2016**, *138*, 11633–11642.
- (22) Raghupathy, R.; Anilkumar, A. A.; Polley, A.; Singh, P. P.; Yadav, M.; Johnson, C.; Suryawanshi, S.; Saikam, V.; Sawant, S. D.; Panda, A. Transbilayer Lipid Interactions Mediate Nanoclustering of Lipid-Anchored Proteins. *Cell* **2015**, *161*, 581–594.
- (23) Cheng, X.; Smith, J. C. Biological Membrane Organization and Cellular Signaling. *Chem. Rev.* **2019**, *119*, 5849–5880.
- (24) Polley, A.; Mayor, S.; Rao, M. Bilayer Registry in a Multicomponent Asymmetric Membrane: Dependence on Lipid Composition and Chain Length. *J. Chem. Phys.* **2014**, *141*, No. 064903.
- (25) Wang, Q.; London, E. Lipid Structure and Composition Control Consequences of Interleaflet Coupling in Asymmetric Vesicles. *Biophys. J.* **2018**, *115*, 664–678.
- (26) Tian, J.; Nickels, J. D.; Katsaras, J.; Cheng, X. Behavior of Bilayer Leaflets in Asymmetric Model Membranes: Atomistic Simulation Studies. *J. Phys. Chem. B* **2016**, *120*, 8438–8448.
- (27) Galimzyanov, T. R.; Molotkovsky, R. J.; Bozdaganyan, M. E.; Cohen, F. S.; Pohl, P.; Akimov, S. A. Elastic Membrane Deformations Govern Interleaflet Coupling of Lipid-Ordered Domains. *Phys. Rev. Lett.* **2015**, *115*, No. 088101.
- (28) Perlmuter, J. D.; Sachs, J. N. Interleaflet Interaction and Asymmetry in Phase Separated Lipid Bilayers: Molecular Dynamics Simulations. *J. Am. Chem. Soc.* **2011**, *133*, 6563–6577.
- (29) Eicher, B.; Marquardt, D.; Heberle, F. A.; Letofsky-Papst, I.; Rechberger, G. N.; Appavou, M.-S.; Katsaras, J.; Pabst, G. Intrinsic Curvature-Mediated Transbilayer Coupling in Asymmetric Lipid Vesicles. *Biophys. J.* **2018**, *114*, 146–157.
- (30) Haataja, M. P. Lipid Domain Co-Localization Induced by Membrane Undulations. *Biophys. J.* **2017**, *112*, 655–662.
- (31) London, E. Membrane Structure–Function Insights from Asymmetric Lipid Vesicles. *Acc. Chem. Res.* **2019**, *52*, 2382–2391.
- (32) Lin, X.; Zhang, S.; Ding, H.; Levental, I.; Gorfe, A. A. The Aliphatic Chain of Cholesterol Modulates Bilayer Interleaflet Coupling and Domain Registration. *FEBS Lett.* **2016**, *590*, 3368–3374.
- (33) Thallmair, S.; Ingólfsson, H. I.; Marrink, S. J. Cholesterol Flip-Flop Impacts Domain Registration in Plasma Membrane Models. *J. Phys. Chem. Lett.* **2018**, *9*, 5527–5533.
- (34) Scheidt, H. A.; Meyer, T.; Niklaus, J.; Baek, D. J.; Haralampiev, I.; Thomas, L.; Bittman, R.; Müller, P.; Herrmann, A.; Huster, D. Cholesterol's Aliphatic Side Chain Modulates Membrane Properties. *Angew. Chem., Int. Ed.* **2013**, *52*, 12848–12851.
- (35) Collins, M. D. Interleaflet Coupling Mechanisms in Bilayers of Lipids and Cholesterol. *Biophys. J.* **2008**, *94*, L32–L34.
- (36) May, S. Trans-Monolayer Coupling of Fluid Domains in Lipid Bilayers. *Soft Matter* **2009**, *5*, 3148–3156.
- (37) Gu, R.-X.; Baoukina, S.; Tielemans, D. P. Cholesterol Flip-Flop in Heterogeneous Membranes. *J. Chem. Theory Comput.* **2019**, *15*, 2064–2070.
- (38) Sodt, A. J.; Sandar, M. L.; Gawrisch, K.; Pastor, R. W.; Lyman, E. The Molecular Structure of the Liquid-Ordered Phase of Lipid Bilayers. *J. Am. Chem. Soc.* **2014**, *136*, 725–732.
- (39) Sodt, A. J.; Pastor, R. W.; Lyman, E. Hexagonal Substructure and Hydrogen Bonding in Liquid-Ordered Phases Containing Palmitoyl Sphingomyelin. *Biophys. J.* **2015**, *109*, 948–955.
- (40) Yang, K.; Shao, X.; Ma, Y.-q. Shape Deformation and Fission Route of the Lipid Domain in a Multicomponent Vesicle. *Phys. Rev. E* **2009**, *79*, No. 051924.
- (41) Izvekov, S.; Voth, G. A. A Multiscale Coarse-Graining Method for Biomolecular Systems. *J. Phys. Chem. B* **2005**, *109*, 2469–2473.
- (42) Wang, Z.-J.; Deserno, M. A Systematically Coarse-Grained Solvent-Free Model for Quantitative Phospholipid Bilayer Simulations. *J. Phys. Chem. B* **2010**, *114*, 11207–11220.
- (43) Marrink, S. J.; Risselada, H. J.; Yefimov, S.; Tielemans, D. P.; De Vries, A. H. The Martini Force Field: Coarse Grained Model for Biomolecular Simulations. *J. Phys. Chem. B* **2007**, *111*, 7812–7824.
- (44) Bussi, G.; Donadio, D.; Parrinello, M. Canonical Sampling through Velocity Rescaling. *J. Chem. Phys.* **2007**, *126*, No. 014101.
- (45) Parrinello, M.; Rahman, A. Polymorphic Transitions in Single Crystals: A New Molecular Dynamics Method. *J. Appl. Phys.* **1981**, *52*, 7182–7190.
- (46) Huang, J.; Rauscher, S.; Nawrocki, G.; Ran, T.; Feig, M.; de Groot, B. L.; Grubmüller, H.; MacKerell, A. D., Jr Charmm36m: An Improved Force Field for Folded and Intrinsically Disordered Proteins. *Nat. Methods* **2017**, *14*, 71–73.
- (47) Jo, S.; Kim, T.; Iyer, V. G.; Im, W. Charmm-Gui: A Web-Based Graphical User Interface for Charmm. *J. Comput. Chem.* **2008**, *29*, 1859–1865.
- (48) Lee, J.; Cheng, X.; Swails, J. M.; Yeom, M. S.; Eastman, P. K.; Lemkul, J. A.; Wei, S.; Buckner, J.; Jeong, J. C.; Qi, Y. Charmm-Gui Input Generator for Namd, Gromacs, Amber, Openmm, and Charmm/Openmm Simulations Using the Charmm36 Additive Force Field. *J. Chem. Theory Comput.* **2016**, *12*, 405–413.
- (49) Essmann, U.; Perera, L.; Berkowitz, M. L.; Darden, T.; Lee, H.; Pedersen, L. G. A Smooth Particle Mesh Ewald Method. *J. Chem. Phys.* **1995**, *103*, 8577–8593.
- (50) Nosé, S. A Molecular Dynamics Method for Simulations in the Canonical Ensemble. *Mol. Phys.* **1984**, *52*, 255–268.
- (51) Hoover, W. G. Canonical Dynamics: Equilibrium Phase-Space Distributions. *Phys. Rev. A: At., Mol., Opt. Phys.* **1985**, *31*, 1695.

- (52) Hess, B.; Bekker, H.; Berendsen, H. J.; Fraaije, J. G. Lincs: A Linear Constraint Solver for Molecular Simulations. *J. Comput. Chem.* **1997**, *18*, 1463–1472.
- (53) Abraham, M. J.; Murtola, T.; Schulz, R.; Páll, S.; Smith, J. C.; Hess, B.; Lindahl, E. Gromacs: High Performance Molecular Simulations through Multi-Level Parallelism from Laptops to Supercomputers. *SoftwareX* **2015**, *1*, 19–25.
- (54) Weiner, M. D.; Feigenson, G. W. Presence and Role of Midplane Cholesterol in Lipid Bilayers Containing Registered or Antiregistered Phase Domains. *J. Phys. Chem. B* **2018**, *122*, 8193–8200.